Structure and Dynamic Properties of Diunsaturated 1-Palmitoyl-2-Linoleoyl-*sn*-Glycero-3-Phosphatidylcholine Lipid Bilayer from Molecular Dynamics Simulation

Marja T. Hyvönen,* Tapio T. Rantala,* and Mika Ala-Korpela#
*NMR Research Group, Department of Physical Sciences, University of Oulu, Oulu, and the #A. I. Virtanen Institute for Molecular Sciences, University of Kuopio, Kuopio and Wihuri Research Institute, Helsinki, Finland

ABSTRACT Unsaturated fatty acid chains are known to be an essential structural part of biomembranes, but only monounsaturated chains have been included in the molecular dynamics (MD) simulations of membrane systems. Here we present a 1-ns MD simulation for a diunsaturated 1-palmitoyl-2-linoleoyl-sn-glycero-3-phosphatidylcholine (PLPC; 16:0/18:2$^{\Delta 9,12}$) bilayer. The structural behavior of the phosphatidylcholine headgroup, the glycerol backbone, and the hydrating water were assessed and found to be consistent with the existing information about similar systems from both experimental and computational studies. Further analysis was focused on the structure of the double bond region and the effects of the diunsaturation on the bilayer interior. The behavior of the diunsaturated sn-2 chains is affected by the tilted beginning of the chain and the four main conformations of the double bond region. The double bonds of the sn-2 chains also influenced the characteristics of the saturated chains in the sn-1 position. Furthermore, extreme conformations of the sn-2 chains existed that are likely to be related to the functional role of the double bonds. The results here point out the importance of polyunsaturation for the biological interpretations deduced from the membrane MD simulations.

INTRODUCTION

Phospholipid molecules are the main building blocks of biological membrane structures. It has become evident that the phospholipid matrix is not simply a solvent for the protein components but an independent regulator of the function of many proteins (Mouritsen and Kinnunen, 1996). The flexibility provided by varying lipid composition and the saturation state of fatty acids characterize mono- and bilayers in biological systems. It is interesting to note, however, that some degree of unsaturation always seems to be present (Cullis and Hope, 1985). This is undoubtedly a sign of the crucial role of the double bonds for the structure and function of biomembranes.

The effects of molecular composition on the general physical properties, such as acyl chain order and phase transition temperature, have been extensively studied, and a lot of specific information exists, for example, about the effects of different phospholipid species and cholesterol on the membrane structure and dynamics (Seelig and Seelig, 1980). It is also clear that the variation in the physical properties of membranes with different degrees of unsaturation cannot simply be explained by the differences in the transition temperatures (Lafleur et al., 1990). Recent studies have also pointed out the importance of phospholipid polyunsaturation on the local properties of membranes, such as specific lipid-protein interactions and lateral domain formation (Slater et al., 1996).

Received for publication 19 February 1997 and in final form 25 August 1997.

Address reprint requests to Dr. Mika Ala-Korpela, Wihuri Research Institute, Kalliolinnantie 4, 00140 Helsinki, Finland. Tel.: 358-9-6223391; Fax: 358-9-637476; E-mail: mika.ala-korpela@csc.fi.

0006-3495/97/12/2907/17 $2.00

It is thus becoming evident that understanding of membrane functions calls for structural and dynamic information about the membrane constituents at an atomic level, e.g., the structural characteristics of double bonds and their effects on the membrane interior. There are many difficulties that limit experimental information on complex and dynamic membrane structures. For instance, even though x-ray and neutron diffraction methods are powerful tools to obtain general structural information on biomembranes, they are less suitable in revealing local structural details. In contrast, the data obtained by deuterium nuclear magnetic resonance (^{2}H NMR) are much better suited for the analysis of atomic level phenomena in the membranes, such as the local orientational order parameters (S^{CD}) of specific carbon segments in the fatty acid chains. However, the interpretation of these parameters is not straightforward due to the orientational dynamics. Thus, it is often problematic to figure out the local conformations that may be responsible for the observed S^{CD} values. Due to the tedious nature of specific deuteration experiments, many ^{2}H NMR measurements of membrane S^{CD} values rely on perdeuterated phospholipid compounds, in which all of the protons of a fatty acid chain are replaced with deuterons. This leads to smoothed orientational order profiles (Lafleur et al., 1989; McCabe et al., 1994; Holte et al., 1995), which provide a good measure of the general behavior but are not able to describe the local variations due to heavily overlapping information and an assumption about a monotonic decrease in the orientational order profile of the fatty acid chain.

The experimental limitations have led to increased implementation of computational methods into the studies of biomembranes. Although molecular dynamics (MD) and Monte Carlo simulations at the atomic level provide an advanced tool to look at the local membrane structure, simpler models can also be applied, for example, to char-

acterize large-scale cooperative phenomena in membranes (Merz and Roux, 1996). The MD simulations, using empirical force fields to describe the atomic interactions, have been extensively used in the investigations of proteins (Brooks et al., 1988). Increased biochemical interest in the behavior of lipid systems, together with the improvements both in the methodology and in the computational resources, have led to an increasing number of MD studies of biomembranes. Mostly, MD simulations have been applied to pure phospholipid systems, including studies of mono- and bilayers and micelles (Alper et al., 1993; Chiu et al., 1995; Damodaran and Merz, 1994; Egberts et al., 1994; Essmann et al., 1995; Heller et al., 1993; Robinson et al., 1994; Shinoda et al., 1995; Stouch, 1993; Tu et al., 1995; Venable et al., 1993; Wendoloski et al., 1989). Recently, also studies in which cholesterol, model peptides, or proteins have been incorporated into the phospholipid systems have been carried out (Robinson et al., 1995; Roux and Karplus, 1993; Damodaran et al., 1995; Edholm et al., 1995). Additionally, simulation approaches have been used to address the questions of diffusion across the bilayer (Marrink and Berendsen, 1994; Wilson and Pohorille, 1996; Bassolino-Klimas et al., 1993, 1995). The studies have shown that many characteristic parameters produced by the MD simulations are consistent with available experimental data. As an important consequence, the novel results provided by the MD simulations can be considered as independent information about the biomembrane structure and dynamics without direct comparison with experiments.

The simulated membranes have mostly been assembled using saturated phospholipid molecules, except for the simulations of 1-palmitoyl-2-oleoyl-*sn*-glycero-3-phosphatidylcholine (POPC, 16:0/18:$1^{\Delta 9}$) (Heller et al., 1993), 1,2-dioleoyl-*sn*-glycero-3-phosphatidylcholine and 1,2-dioleoyl-*sn*-glycero-3-phosphatidylethanolamine (DOPC and DOPE, 18:$1^{\Delta 9}$/18:$1^{\Delta 9}$) systems (Huang et al., 1994). In this work we present a detailed analysis for the 1-ns MD simulation of a 1-palmitoyl-2-linoleoyl-*sn*-glycero-3-phosphatidylcholine (PLPC, 16:0/18:$2^{\Delta 9,12}$) bilayer, which contains biologically representative fatty acids (Op den Kamp et al., 1985; Esterbauer et al., 1990). The study is focused on the structure of the double bond region of the sn-2 fatty acids and on the effects of the two *cis* double bonds on the membrane characteristics. Additionally, we provide specific information on the atomic distributions and the behavior of hydrating water molecules, phosphatidylcholine (PC) headgroups, and the glycerol backbones. The simulation revealed novel characteristics due to the two double bonds and pointed out the importance of incorporating polyunsaturation into the biomembrane simulations when aiming toward more realistic biological interpretations.

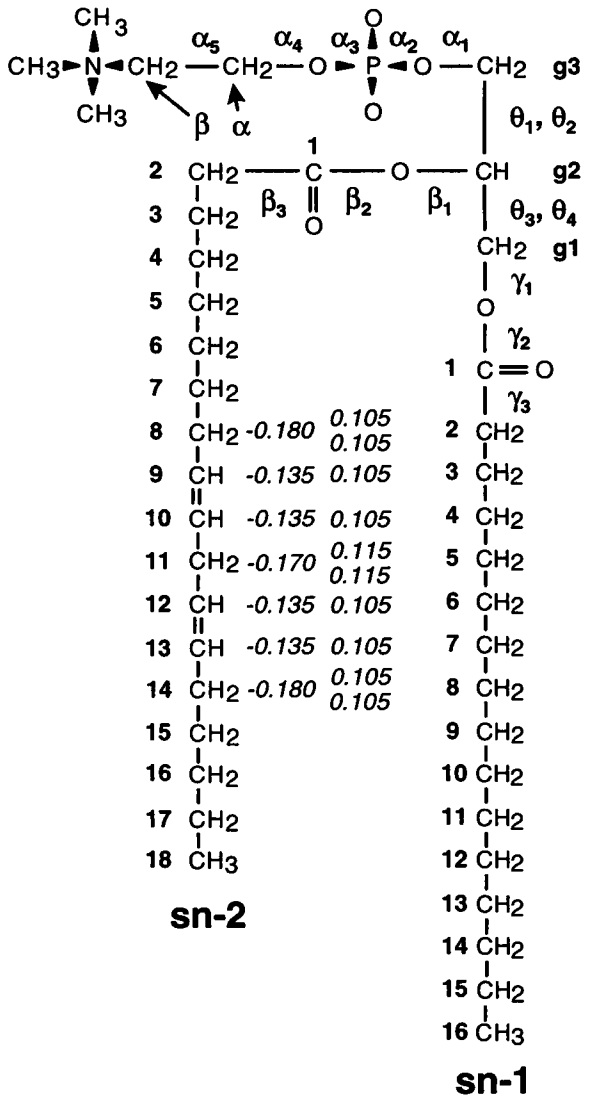

FIGURE 1 The structure of a single PLPC molecule together with the identification of the dihedral angles and the numbering of the carbon atoms. The partial charges (in units of *e*) of the double bond region are also shown.

METHODS

Modeling and computational details

A PLPC molecule, shown in Fig. 1, consists of a glycerol backbone (Cg1-Cg3) into which the saturated palmitic acid chain (16:0), the diunsaturated linoleic acid chain (18:$2^{\Delta 9,12}$), and the PC headgroup are attached to the positions sn-1, sn-2, and sn-3, respectively. The PLPC was built up with the two double bonds in *cis* and the other chain bonds in *trans* configuration after which the energy was minimized. The layer construction was started by placing four identical PLPC molecules into a square-like configuration with the headgroups pointing up along the *y* axis. Each PLPC was given a different orientation in the *x*-*z* plane to avoid collective tilting and to ensure the formation of a liquid crystalline phase. A surface area of 8.4 × 8.4 Å^2 per PLPC molecule was used based on x-ray scattering experiments for membranes with various lipid compositions (Lewis and Engelman, 1983). The block of four PLPC molecules was stabilized by an energy minimization and a dynamic heating-annealing cycle using periodic boundary conditions (PBCs) in the *x*-*z* plane. Such blocks were added together to form a 4 × 4 grid, which was stabilized in the above manner. Finally, five more blocks were added and the energy minimized. This resulted in a monolayer of 36 PLPC molecules in a grid with an area of 50.4 × 50.4 Å^2. The monolayer was solvated by placing an equilibrated water box of 50.4 × 22.0 × 50.4 Å^3 (density ≈ 1 kg/dm^3) so that it overlapped the headgroup region. This ensured that the void volume between the headgroups was filled with water. The water molecules over-

lapping the PLPC molecules were then removed, resulting in a model system consisting of 36 PLPC and 1368 water molecules (in all, 8856 atoms). This monolayer system had the dimensions of 50.4 Å × 36.75 Å × 50.4 Å in x, y, and z directions, respectively.

The 36-molecule piece of the monolayer was used to model an infinite bilayer by applying suitable symmetry operations and PBCs. First, the bilayer was modeled with a 180° rotation about an axis parallel to the x axis and a further 90° rotation about the y axis, resulting in a rotary-reflection S_4 about the y axis (plus a redundant reflection). The first rotation axis was chosen to result in a phosphorus-to-phosphorus distance of 37 Å, which was estimated from the experiments (Lewis and Engelman, 1983). Second, at the x-z plane, conventional PBCs were used to model an infinite bilayer. The final energy minimization was reached by first stabilizing the water molecules and then the whole system. A 10-ps dynamic heating period up to the temperature of 310 K was performed and followed by an equilibration period of 200 ps. Velocities were scaled once at t = 33 ps from the start of the equilibration, because of a drift in the temperature. Furthermore, the simulation was carried out for 1 ns to collect the data reported here. The primary model system (i.e., the 36-molecule piece of the monolayer) is shown as a snapshot from the simulation in Fig. 2. The simulation was performed in a microcanonical (constant volume and energy) ensemble. The temperature and the energies were monitored during the simulation to ensure their stability and the adequate length of the equilibration. The average temperature in the 1-ns simulation was 321 K, which is well above the gel-to-liquid-crystal phase transition temperature of the PLPCs (Niebylski and Salem Jr., 1994).

The simulation was performed applying the CHARMm software (CHARMm version 22.2). Lipid force field parameters were used (Schlenkrich et al., 1996, personal communication), except for the double bond region of the linoleic acid, which was not available in the parameter set. Thus, the partial charges of this region (shown in Fig. 1) were estimated by an ab initio local density functional calculation (DMol, version 2.3) (charges partitioned using the method of Hirshfeld, 1977) and adapted to the charge distribution of the rest of the molecule. Other parameters for the double bond region were obtained from the CHARMm parameter set for amino acids. For water molecules, the TIP3P parameters (Jorgensen et al., 1983) were used. All atoms were independently taken into account in the MD simulation. The lengths of the bonds involving hydrogen atoms were fixed using the SHAKE algorithm, which allowed using a 1-fs time step (van Gunsteren and Berendsen, 1977). Long-range interactions were truncated using a group-based cutoff radius of 13 Å with a shifting function for the electrostatic and a switching function for the van der Waals interactions (Brooks et al., 1983). The nonbonded interactions were updated every 25th step (0.025 ps) during the heating and the first 80 ps of equilibration after which update was performed every 10th step, which was enough to maintain constant energy. Energies, coordinates, and velocities were saved every 25th step. The simulation was carried out using SGI Power Challenge (5 h CPU/1 ps) and Cray C94 (9 min CPU/1 ps) computers.

Data analysis

In the subsequent analysis, the averages have been calculated over all saved time steps (40,000) and over all PLPC or water molecules, if not described otherwise.

Atomic single particle distribution functions in the bilayer normal direction were evaluated by calculating the total amount of each atom in 0.25-Å-thick slices. The distributions were averaged over time. Furthermore, they were used to calculate the mass density profiles for the main components of the bilayer and the total mass and electron density across the bilayer. Radial distributions of the oxygen and hydrogen atoms of the water molecules around the phosphorus and nitrogen atoms of the PC headgroups were averaged from the last 10 ps of the simulation using the SCARECROW software (Laaksonen, 1992). The mean cosine of the angle between the water dipole moment vector and the bilayer normal in 0.25-Å slices along the bilayer normal was also calculated. A zero value is obtained for a random orientation, and a negative value corresponds the orientation of the dipole toward the bilayer center. Orientation angle of the headgroup and glycerol backbone with respect to the bilayer normal as well as the angle distributions were determined using 1° slices.

The fractions of *gauche*$^+$ (g^+), *gauche*$^-$ (g^-), and *trans* (t) states were determined for the dihedral angles of the glycerol backbone, the headgroup, and both chains. The division into these three states was performed using the ranges −120–0 and 0–120° for the g^+ and g^- states, respectively, and the rest for the t states. Similar division was used in the evaluation of the rate of isomerization between g^+, g^-, and t states for each bond. The isomerization rate was averaged over molecules.

The orientational order is described by the order parameter S_j, which is defined as

$$S_j = \tfrac{1}{2}\langle 3\cos^2\beta_j - 1\rangle, \quad (1)$$

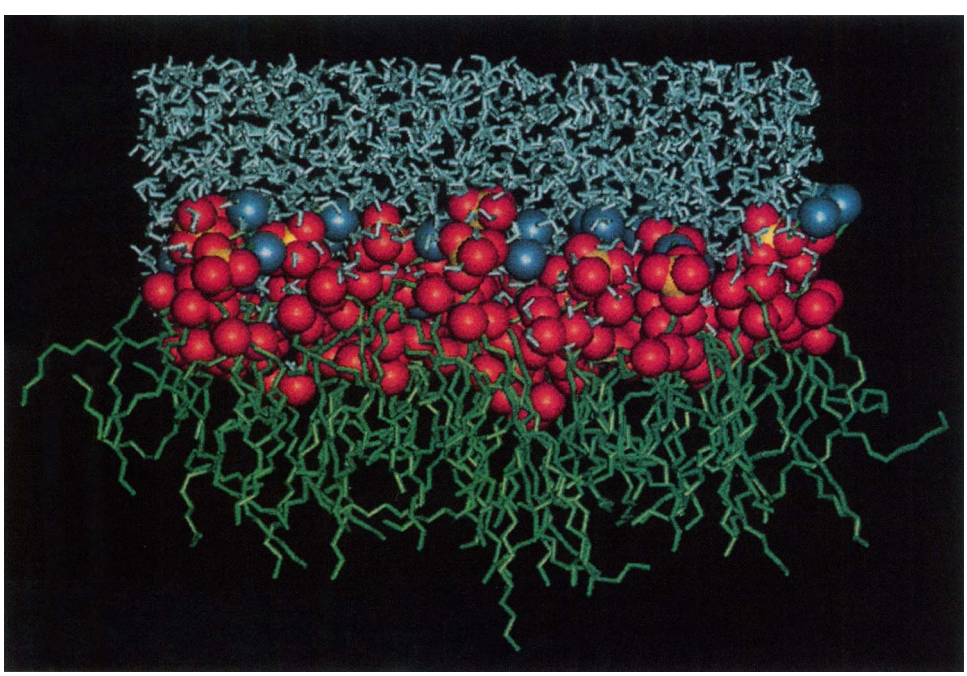

FIGURE 2 A snapshot from the end of the simulation showing the upper half of the bilayer (i.e., the primary simulation box). The water molecules are shown in cyan and the color coding of the PLPC molecules is as follows: green for carbon, red for oxygen, yellow for phosphorus, and blue for nitrogen. For clarity, the hydrogens of the PLPC molecules are not shown. The y direction is along the normal of the membrane.

where β_j is the angle between the orientation vector and the reference direction. The brackets denote both the ensemble and time average. A ^2H NMR observable order parameter, S_j^{CD}, is obtained by defining the orientation vector along the CH_j bond and the bilayer normal as the reference direction. According to this definition we calculated the order parameters from the PLPC simulation for the two CH bonds, CH_{aj} and CH_{bj}, at each saturated carbon atom in the chains. As an error estimation, the standard error of mean (SEM) of the 36 molecular averages is given. For each of the molecules, the molecular average was evaluated from the whole time series of 1 ns. In this way, the effect of high correlation between consecutive time steps is eliminated, which results in more realistic error estimates. It is conventional in MD simulations to define the orientation vector along the normal of the HC_jH plane or from C_{j-1} to C_{j+1}, which leads to the molecular order parameter S_j^{mol}. When isotropic rotations around the HC_jH plane normal are assumed, the CH bonds and corresponding S_j^{CD} values become equivalent, and S_j^{CD} can be compared with the S_j^{mol} values according to the relation $-2S_j^{CD} = S_j^{mol}$ (Seelig and Niederberger, 1974). The S_j^{mol} may vary between -0.5 and 1 corresponding to the variation between perpendicular (90°) and parallel (0°) orientation with respect to the bilayer normal. Usually, the zero value of S_j indicates isotropic orientation distribution but also, e.g., a single orientation angle of 54.7° in the sample results in the zero value.

The reduced temperature θ, i.e., the temperature of a system with respect to the gel-to-liquid-crystalline phase transition temperature T_m, is defined as

$$\theta = \frac{T - T_m}{T_m}, \qquad (2)$$

where T is the temperature of the system.

The root mean square (RMS) fluctuations were calculated for each carbon segment of the chains. In addition, the orientational angle distributions of varying bonds and vectors in the chains were calculated with respect to the bilayer normal. Note that here the bilayer normal was considered to point toward the bilayer center, in contrast to the determination of orientational distributions in the headgroup and glycerol backbone region. This was done to keep the numerical values mainly below 90°. For the two single bonds between the double bonds, the values of the dihedral angles were monitored during the simulation and the angle distributions determined. The percentage fraction of conformations with different combinations of these angles was also determined.

Due to the symmetry operations used to model the bilayer, the tails of the PLPC molecules may occasionally be close to their images at the center of the simulation box. To check that there was no significant bias between the inner and outer regions, the average atomic distributions of representative atoms in the head group (N, P), glycerol backbone (Cg2), sn-1 (C8, C15), and sn-2 chain (C8, C17) were calculated separately from equal volumes, which were determined by dividing the area in the x-z plane equally into an inner square and an outer part. The orientational order parameters for C8 and C15 of the sn-1 chain and for C8 and C17 of the sn-2 chain were also calculated from these inner and outer volumes. No significant differences were noticed between the corresponding averages (data not shown).

RESULTS AND DISCUSSION

General aspects

There are many reports of simulations for saturated phospholipid bilayers in the literature, but surprisingly, the unsaturation has been taken into account only in the simulations of phospholipids with monounsaturated sn-2 chains (Heller et al., 1993) or both chains (Huang et al., 1994). The current work is, to our knowledge, the first simulation of a bilayer consisting of biologically common polyunsaturated phospholipids with saturated sn-1 and diunsaturated sn-2 chain. The main focus of this study was the structure of the double bond region and the effects of the diunsaturation on the bilayer interior. As the structure of the PC headgroup, the glycerol backbone, and the hydrating water has been widely investigated both experimentally and computationally, the evaluation of these properties and the comparison with existing information provided a sound basis for the further investigation of the diunsaturated chains and their effects on the sn-1 chain, for which reference data are more difficult to find.

The atomic single particle distribution functions and average positions in the bilayer normal (y) direction were calculated and are shown in Fig. 3. They provide general information on the structure of the system. The glycerol backbone and the beginning of the sn-2 chain have the narrowest distributions, implying that they are the most rigid parts when motions in the y direction are considered. In general, the width of the distributions for the chain

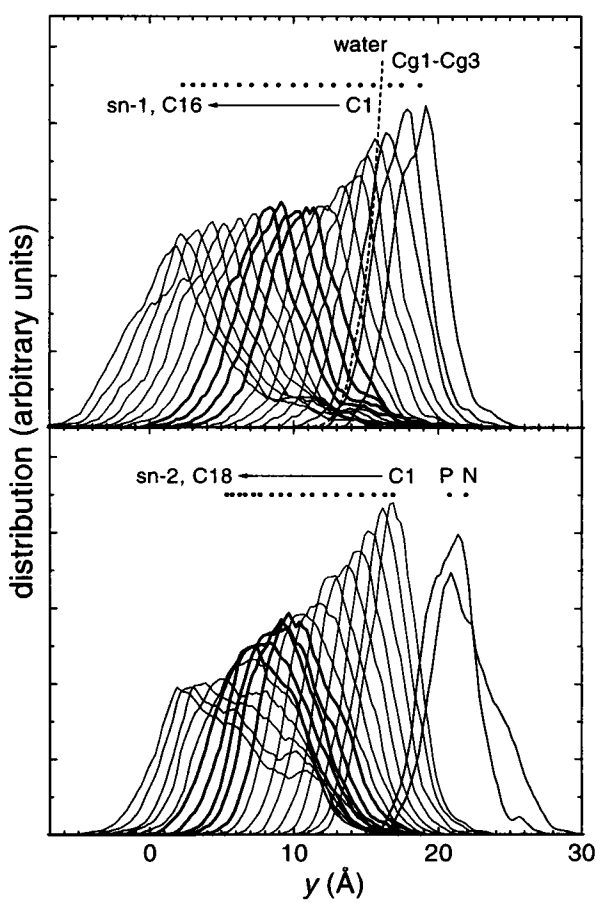

FIGURE 3 Atomic distributions along the bilayer normal (y). In the upper panel are shown the sn-1 chain carbons, water (- - -) and glycerol backbone carbons (Cg1-Cg3); in the lower panel are the sn-2 chain carbons, phosphorus and nitrogen. The distributions of the sn-2 double bond region carbons (C9-C13) are drawn in bold together with the carbons C6-C9 of the sn-1 chain, which lie approximately at the same height in the layer with the double bonds. Also, average positions for each atom are shown (●). Note that the center of the bilayer is at zero and that the scales are the same in both figures.

carbons increase toward the center of the bilayer. The distribution of the nitrogen atoms is also slightly wider than the one for the phosphorus atoms. These observations are consistent with the x-ray and neutron diffraction results of DOPC (Wiener and White, 1992), which indicate the glycerol region to be the most rigid part of a liquid crystalline phospholipid bilayer. Generally, the distributions are wider in the simulation than the ones based on the x-ray and neutron diffraction results of DOPC. This is possibly due to the relatively low hydration of the DOPC bilayer in the experiments; along the hydration, the effective size of the polar headgroup increases, the lateral packing of the chains loosens, and the thermal motion increases (Wiener and White, 1992; Lehtonen and Kinnunen, 1994).

The average phosphorus-phosphorus distance across the bilayer during the simulation was 41.6 Å. There was no quantitative value for the P-P distance in the case of the PLPC system in the literature, and thus for the construction, the initial value of 37 Å was estimated based on experimental data from a selection of PC systems (Lewis and Engelman, 1983). The final value for the average P-P distance was achieved during the equilibration. An experimental value of approximately 40.4 Å for a DOPC system (Wiener and White, 1992) would imply that the PLPC bilayer in our simulation could be slightly too thick. However, this is a complex matter depending on the hydration, temperature, and degree of unsaturation, and furthermore, quantitative experimental data that would systematically assess the contribution of these factors seem not to exist. Of course, in the simulation, many of the approximations used can have an effect, but currently it is difficult to assess their individual contribution on the bilayer thickness.

The distributions reveal the nonparallel average orientation of the glycerol backbone and the P-N vector of the headgroup with respect to the bilayer surface. The vertical displacement of the average positions for the Cg1 and Cg2 carbons of the glycerol backbone was 0.8 Å. Interestingly, the same average value has been concluded by Eklund et al. (1992) from fluorescence spectroscopic measurements (using pyrene labels in both chains of PC species). It is also notable that, as the atomic distributions at the double bond region (C9-C13) overlap with the distributions of the sn-1 carbons C6-C9, these fragments in the sn-1 chains are most directly affected by the double bonds. Furthermore, in the sn-1 chains the spacing between the average positions of the fragments remains almost constant toward the end of the chains, but in the sn-2 chains the spacing decreases after the double bonds. This is an indication of the existence of tilted conformations at the end of the sn-2 chains.

The total mass density and electron density profiles can be approximated with good accuracy as the atomic positions are known. They were calculated from the distributions of atoms in the bilayer normal direction and are shown in Fig. 4 together with the mass density profiles for the main components of the system. The mass (electron) density maximum of 1.35 kg/dm^3 (0.44 e/Å^3) at ~20–22 Å is approximately at the height of phosphorus and nitrogen, and

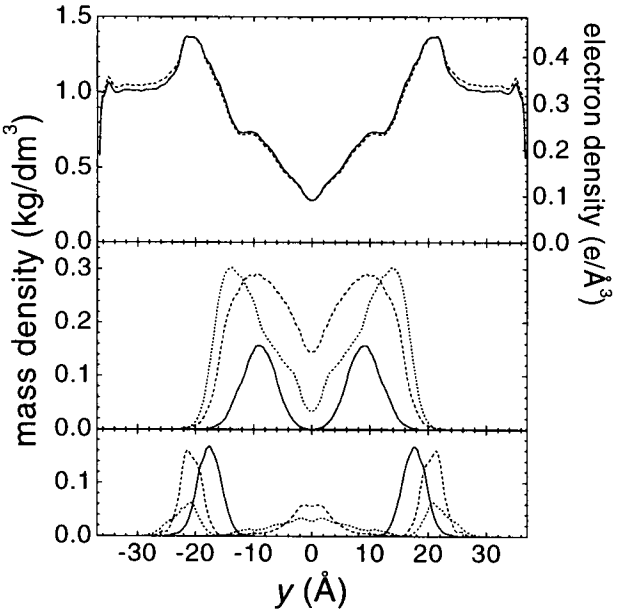

FIGURE 4 Density profiles along the bilayer normal (y). The top panel shows the total mass (——) and electron density (- - -) profile; in the middle are the mass density profiles for the methylene carbons of the sn-1 chain (- - -), together with the methylene (· · ·) and double-bonded carbons (——) of the sn-2 chain; on the bottom are the mass density profiles for the nitrogen (· · ·), phosphorus (- - -), glycerol backbone carbons (——), and the methyl carbons of the sn-1 (- - -) and sn-2 (· · ·) chains. The center of the bilayer is at zero.

the minimum of 0.28 kg/dm^3 (0.09 e/Å^3) in the center of the bilayer. From 20 Å to 13 Å the mass density steadily decreases toward the short plateau of 0.73 kg/dm^3 at the height of the sn-1 carbons C5-C7 and the sn-2 carbons C7-C9. Interestingly, the plateau density is very close to the density of liquid hexadecane (0.77 kg/dm^3 at 20°C) especially when thermal expansion is taken into account. A similar plateau density was observed in the mass density profile of 1,2-dipalmitoyl-*sn*-glycero-3-phosphatidylcholine (DPPC) in a MD simulation (Egberts et al., 1994). Approximately at the height of the beginning of the PLPC chains the density is 1.10 kg/dm^3, which is consistent with the findings of Egberts at al. (1994) for DPPC. However, in the bilayer center they reported a density of 0.60 kg/dm^3, which is much higher than what is observed here for the PLPC bilayer. The shape of the profiles for the PLPC from the simulation is remarkably similar to the x-ray density profiles of DPPC and POPC (McIntosh and Simon, 1986; Wiener and White, 1992).

Lateral packing of the headgroup and fatty acid chains was also assessed. The PC headgroups had a tendency to arrange in pairs or chains to compensate the headgroup dipoles (data not shown). Litman et al. (1996) have suggested for highly unsaturated phospholipids that the chains would pack nonrandomly to maintain maximal saturated sn-1 chain interactions. To test this in our system with lower unsaturation state, the radial distribution for the intermolecular atom pairs C2(sn-1)-C4(sn-2), C2(sn-1)-C2(sn-1), and

C4(sn-2)-C4(sn-2) were determined (data not shown). However, all three distributions had the first peak at ~5.5 Å and thus gave no indication of preferential interactions.

Water, PC headgroup, and glycerol backbone

Distribution of the water molecules

From the distribution of the water molecules shown in Fig. 3 it is seen that the water molecules do not usually penetrate further than the glycerol backbone. It is also seen that the water molecules and the double bond carbons have slightly overlapping distributions. This is in accordance with the x-ray and neutron diffraction results of the DOPC bilayer (Wiener and White, 1992). Due to the wider distributions in the simulation (see above), the overlap is more pronounced according to the simulation than indicated by the experimental results of DOPC. Wiener and White (1992) have also speculated that the overlap may be relevant for the permeability of water molecules and water-soluble small molecules through the bilayer. The water molecules may have transient contacts with the double bonds, which may have contacts over the bilayer center (the distributions range to the bilayer center); the movements of the double bonds can thus be seen to provide a ferry mechanism that could help the water molecules to permeate across the bilayer. Indeed, there is some evidence for enhanced permeability of small molecules due to the incorporation of double bonds into the sn-2 chains (Demel et al., 1972; van Deenen et al., 1972; Fettiplace and Haydon, 1980; Petersen, 1983). In the current simulation, however, no water molecules were observed below 9.4 Å. Some water molecules were observed to penetrate to the height of approximately 11 Å as a result of hydrogen bonding to a PLPC molecule that moved toward the center of the bilayer. These water molecules were transiently hydrogen bonded to each other and to the sn-2 carbonyl of the particular PLPC molecule. This PLPC molecule had the sn-1 chain carbonyl at a lower height than the sn-2 chain carbonyl, and briefly, one water molecule visited also at the height of the sn-1 carbonyl at 9.4 Å.

Radial distribution of water around the PC headgroup

Radial distributions of the oxygen and hydrogen atoms of the water molecules were calculated around the phosphorus and nitrogen atoms of the PC headgroup and are shown in Fig. 5. The water molecules are found to be strongly oriented around the phosphorus atom due to hydrogen bonding between the oxygens of the phosphatidyl group and the hydrogens of the water molecules. The first hydrogen and oxygen layers are at 2.8 Å and 3.8 Å, respectively. Only a weak orientation can be noticed around the nitrogen atom despite the positive charge of the choline group. This is most likely due to the hydrophobic nature of the surrounding methyl groups, which causes the water molecules to form hydrogen bonds among themselves. However, a slight preference for the water oxygens to orient toward the nitrogen is seen; the first peak for the oxygens is at 4.2 Å whereas for the hydrogens it is at 4.4 Å.

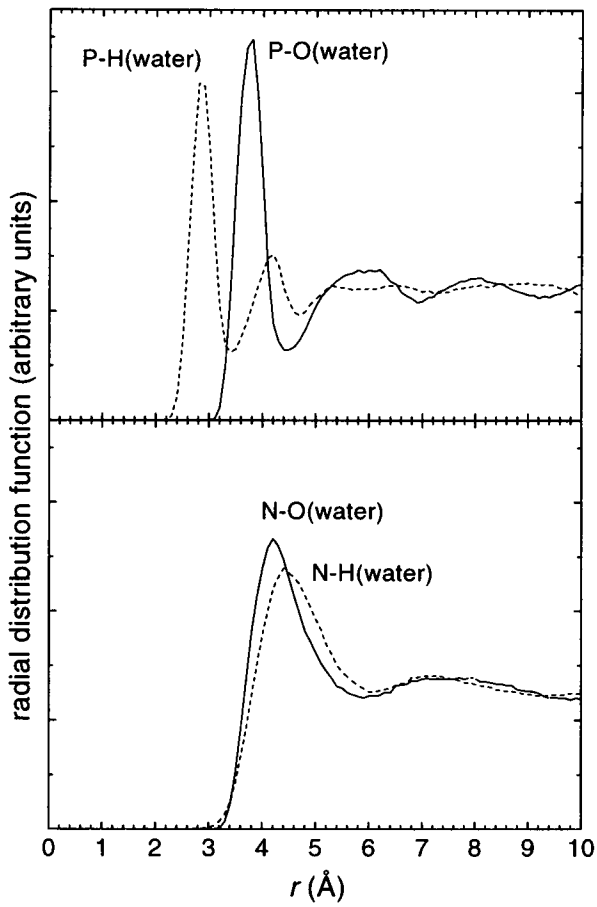

FIGURE 5 Radial distribution functions for the oxygen (——) and hydrogen (- - -) atoms of water molecules around the PLPC phosphorus (*top*) and nitrogen (*bottom*) atoms. The data were averaged from the last 10 ps. Due to the anisotropic system the radial distribution function does not approach one at the long separation limit and therefore it is shown here in arbitrary units.

A very similar arrangement of the water molecules around the PC headgroup has been observed also in other MD simulations (Alper et al., 1993; Damodaran and Merz, 1994; Essmann et al., 1995). However, an even slighter preference of the water oxygens to orient toward the nitrogen was observed by Essmann et al. (1995), and Damodaran and Merz (1994) did not observe any preference. The slight differences between the results are likely due to the different water models used in the simulations.

Orientation of the water dipole with respect to the bilayer normal

The profile for the mean cosine of the angle between the water dipole moment vector and the bilayer normal was calculated and is shown in Fig. 6. It is seen that at the bilayer surface the water dipoles tend to orient toward the bilayer interior. This is due to the strong orientation of the

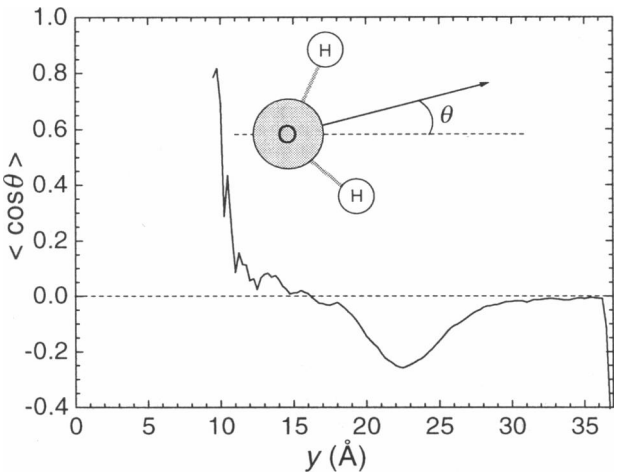

FIGURE 6 The mean cosine of the angle between the water dipole moment vector and the bilayer normal (y). The center of the bilayer is at zero.

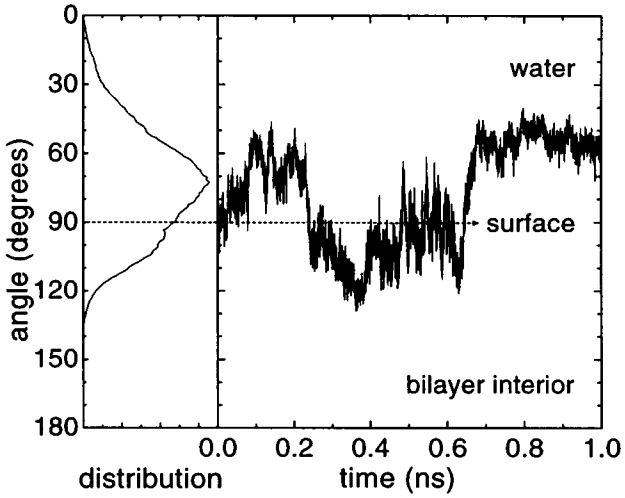

FIGURE 7 The averaged distribution of the orientation angle between the phosphorus-nitrogen vector and the bilayer normal (*left*) together with the time series of the orientation angle for one of the PLPC molecules (*right*).

water hydrogens toward the phosphorus atoms, as indicated by the radial distribution functions (Fig. 5); as the amount of water molecules is larger toward the water phase, the dominating orientation of water dipoles is toward the bilayer center. Similar orientational behavior of the water molecules at the bilayer surface has been observed in the MD simulations of DPPC (Marrink et al., 1993) and 1,2-dimyristoyl-*sn*-glycero-3-phosphatidylcholine (DMPC) systems (Chiu et al., 1995). Only a few water molecules penetrate toward the hydrocarbon region, which results in poor statistics and the spiky profile. The mean orientation of the water dipole toward the bilayer center at the bilayer surface has also been concluded by Gawrisch at al. (1992) based on NMR and x-ray investigations. They suggested the first layer of water molecules at the lipid water interface to make the major contribution to the dipole potential. This contribution has also been proposed by Alper et al. (1993) based on the MD simulations of water hydrating a DMPC monolayer.

Orientation of the PC headgroup and glycerol backbone

To monitor the orientation of the PC headgroups during the simulation, the angle of the phosphorus-nitrogen vector with respect to the bilayer normal was determined. The average angle distribution is shown in Fig. 7 together with a time series, as an example, for one of the PLPC molecules. The average orientation angle with respect to the bilayer surface was 14° toward the water region, and the most prevailing angle was 17°. It is also seen that even for an individual PLPC molecule the phosphorus-nitrogen vector may orient variably between the water phase and the interior of the bilayer, which implies a dynamically rough interface for the membrane.

Various experimental methods have been used to estimate the average orientation angle of the headgroup. The main conclusion has been that, on average, the headgroups lie almost parallel to the bilayer surface (Akutsu and Nagamori, 1991; Büldt and Wohlgemuth, 1981; Hauser et al., 1981; Seelig et al., 1977; Seelig and Seelig, 1980). Some values have also been given, for instance, 18° estimated from the NMR and laser Raman studies of DPPC (Akutsu and Nagamori, 1991). In all, the average orientation of the headgroup in the simulated PLPC bilayer is in agreement with the estimations from the experiments.

The orientational order parameters S^{CD} were determined for the headgroup carbon segments Cα and Cβ to get information on the local orientation and to enable comparison with ^{2}H NMR experiments. A value of 0.087 $\pm$ 0.021 for Cα and 0.024 $\pm$ 0.019 for Cβ was obtained. Experimentally the deuterium quadrupolar splittings have been measured for different phospholipid species with varying hydration and temperature (Bechinger and Seelig, 1991; Gally et al., 1975; Tamm and Seelig, 1983; Ulrich and Watts, 1994). The values of Cβ decrease with increasing temperature and are very similar between different lipid species at approximately the same temperature relative to the phase transition temperature T_m (Gally et al., 1975; Tamm and Seelig, 1983). For instance, the S^{CD} values of 0.023 for DPPC (Gally et al., 1975) and 0.027 for DOPC (Ulrich and Watts, 1994) at high temperatures relative to their T_m are in good agreement with the value calculated for PLPC. For Cα the experimental values vary between 0.046 and 0.049 for different species in varying temperatures (Bechinger and Seelig, 1991; Gally et al., 1975; Seelig et al., 1977; Tamm and Seelig, 1983; Ulrich and Watts, 1994). Although the simulation-based value of Cα for PLPC differs from the experimental ones, the difference corresponds to only <2° change in the CD orientation angle β (Eq. 1).

The orientation angle distributions of the glycerol backbone vectors Cg1-Cg3, Cg2-Cg3, and Cg1-Cg2 are shown

with respect to the bilayer normal in Fig. 8. The most prevailing orientation angle of the whole glycerol backbone was approximately 25° from the bilayer normal, but the distribution ranges even to 90°; i.e., also orientations parallel to the surface were present. Similar orientational behavior has also been observed in the MD simulations of a DMPC bilayer (Stouch, 1993). Furthermore, in the present simulation the bond Cg2-Cg3 was, on average, found in a more upward and a more restricted orientation than the Cg1-Cg2 bond.

Dihedral angle isomerization: gauche and trans states

The fractions of *gauche*$^+$ (g^+), *gauche*$^-$ (g^-), and *trans* (t) states were determined for the torsion angles θ_1-θ_4 of the glycerol backbone, α_1-α_5 of the headgroup, and γ_1-γ_3/β_1-β_3 of the sn-1/sn-2 chain beginnings and are shown in Fig. 9.

The most probable states were $t\,g^+\,t\,g^-/t\,g^+\,g^+\,t\,g^-$ for each dihedral angle θ_1-θ_4/α_1-α_5, respectively. The occurrence of these dihedral angles in a single conformation would lead to a structure in which the sn-1 chain begins straight downwards, the sn-2 perpendicularly, and the headgroup straight upwards from the glycerol backbone. Furthermore, in the point of the phosphorus, the headgroup would bend onto the top of the beginning of the sn-2 chain. This is similar to one of the reported crystal structures of DMPC: $t\,g^+\,t\,g^-/t\,g^+\,g^+\,t\,g^-$ (type B) (Pascher et al., 1992). However, in the simulation only 5.8% of all the conformations had this type of sequence, and the other crystal structure, $g^-\,t\,t\,g^-/t\,g^-\,g^-\,t\,g^+$ (type A), was observed to an even lesser extent (1.0%). This indicates that in the liquid crystalline phase the structural states of the glycerol backbone and the headgroup are highly dynamic, but still a relationship with the crystal structures can be found. Especially the glycerol backbones appeared in the crystal-like structures: 37.9% in type B and 21.6% in type A. In the headgroup conformations the crystal-like structures were not seen that frequently; only 13.5% of the headgroup conformations had the torsion sequence of type B and 1.9% of type A.

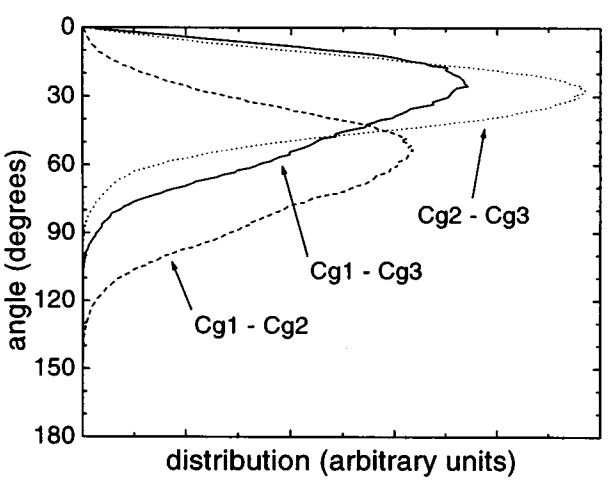

FIGURE 8 The distributions of the angles between the bilayer normal and the glycerol backbone vectors. ——, Cg1-Cg3; - - -, Cg1-Cg2; · · ·, Cg2-Cg3.

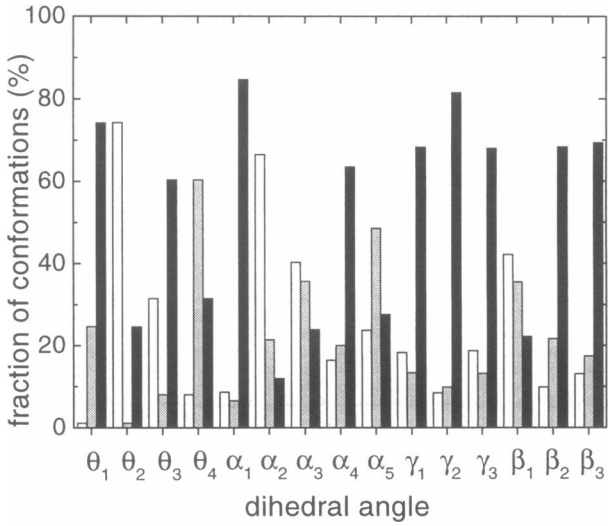

FIGURE 9 The fraction of conformations in *gauche*$^+$ (white), *gauche*$^-$ (gray), and *trans* (black) states for the dihedral angles θ_1–θ_4, α_1–α_5, γ_1–γ_3, and β_1–β_3. The angles are defined in Fig. 1.

The headgroup structures have been studied in the liquid crystalline phase using NMR and laser Raman experiments. Based on the NMR results, Seelig et al. (1977) have suggested $t\,g^+\,g^+\,t\,g^-$ and $t\,g^-\,g^-\,t\,g^+$ sequences for the dihedral angles α_1-α_5 of the headgroup in the liquid crystalline DPPC bilayers. They also suggested rapid transitions between these two conformations. In the simulation the situation was far from being so clear, as these sequences accounted for only 15.4% of all the conformations. Skarjune and Oldfield (1979) could not point out any particular conformations in their study of liquid crystalline DPPC but found families of conformations. Akutsu and Nagamori (1991) proposed, based on ^{2}H NMR and laser Raman studies, the sequences $g^+\,t\,g^-$ and $g^-\,t\,g^-$ for the angles α_3-α_5 as the most reasonable liquid crystalline structures of the choline headgroup. In our simulation they were represented in fractions of 17.1 and 6.8%, respectively. For comparison, the fraction of sequence $g^-\,t\,g^+$ was 6.9%. Taken together, the suggestions based on experiments seem not to converge toward any unique model for the headgroup conformation, but rather give an idea of a variety of prevailing sequences. This kind of behavior is also supported by the results from the present simulation. However, Seelig et al. (1977) stressed that the headgroup structure is characterized by the *gauche-gauche* conformation of α_2-α_3, and Akutsu and Nagamori (1991) pointed out the *gauche* state for α_5. These features clearly coincide with the results from the PLPC simulation.

Hauser et al. (1988) have investigated liquid crystal states of the θ_3/θ_4 angles using ^{1}H NMR and have concluded that the backbone switches mainly between two conformations

t/g^+ and g^-/g^+, of which the t/g^+ is the dominating one. The g^+/t was also detected but with a low population (<10%). In the simulation these three possible conformations were found in the populations of 60.3, 8.1, and 31.6% for the t/g^+, g^-/g^+, and g^+/t, respectively. Thus, the dominating conformation is consistent with the NMR results, but the proportions of the other populations differ from the experimentally observed ones.

The angles γ_1-γ_3 of the sn-1 chain beginning were all mainly in the *trans* states; i.e., the beginning of the sn-1 chain is mostly straight continuation of the glycerol backbone. The β_1 angle was generally in *gauche* state, which indicates that the sn-2 chain beginning was mostly in perpendicular orientation to the glycerol backbone. The downwards bending of the sn-2 chain was then mainly caused by the *gauche* states of the other dihedrals in the beginning of the chain.

The average time period between the transitions was shortest, on the order of 0.5–0.7 ps, for the dihedral angles over the C-O bonds. Transitions over the P-O bonds occurred approximately every 2.0 ps. In comparison, the C-C bonds rotated relatively slowly. The most rigid bond of the glycerol backbone was θ_3, which changes state approximately every 50 ps. These results are consistent with the observation that the major conformational flexibility in the phospholipids is in the C-O and P-O bonds (Sundaralingam, 1972) and that the C-O bonds are more flexible than the P-O bonds (Bicknell-Brown et al., 1982).

Taken together, the present MD simulation results for the PLPC bilayer suggest that the glycerol backbone is more rigid and more crystal-like than the headgroup, for which a variety of dihedral angle sequences were observed. These features are also consistent with the MD simulation results reported for a liquid crystalline DPPC bilayer (Egberts et al., 1994).

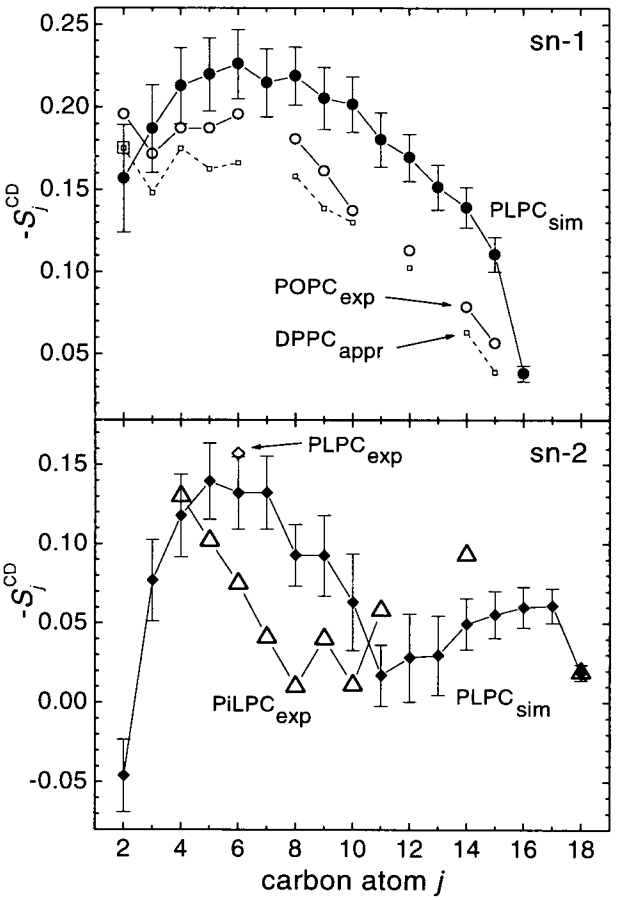

FIGURE 10 The average of the $-S_j^{CD}$ orientational order parameters along the sn-1 (●) and sn-2 (◆) chains of PLPC. For comparison, also the ^{2}H-NMR-based values are shown for the sn-1 chains of a DPPC system (□) (Seelig and Browning, 1978; for the details of the approximation, see text) and of a POPC system (○)(Seelig and Seelig, 1977) together with the values for the sn-2 chains of a PLPC (◇) and PiLPC system (△) (Baenziger et al., 1991). The SEMs of the molecular averages are shown as error bars for the values from the simulation.

sn-1 and sn-2 chains

Orientational order parameters

The averages of the $-S_j^{CD}$ order parameters for each carbon segment of PLPC (16:0/18:2$^{\Delta 9,12}$) are shown in Fig. 10 for the sn-1 and sn-2 chains. DePaked ^{2}H NMR-based smoothed order profiles (Lafleur et al., 1989; Holte et al., 1995) of the saturated sn-1 chains cannot be used as a reference material here, because they describe only the general orientational features and cannot account for detailed local characteristics, particularly for the carbons C2-C8. We are unaware of any reported order parameters for the sn-1 chain of PLPC. So, for comparison, the ^{2}H NMR order parameters of the sn-1 chains in the monounsaturated POPC (16:0/18:1$^{\Delta 9}$) (Seelig and Seelig, 1977) and saturated DPPC (16:0/16:0) (Seelig and Browning, 1978) are shown. Here we have assumed that the phase transition temperature T_m of PLPC is −15°C; i.e., the reduced temperature is θ = 0.24. This is likely to be near the actual one, because the T_m of 1-palmitoyl-2-isolinoleoyl-*sn*-glycero-3-phosphatidylcholine (PiLPC, 16:0/18:2$^{\Delta 6,9}$) is approximately −15°C (Baenziger et al., 1991), and the T_m of SLPC(18:0/18:2$^{\Delta 9,12}$) is −16.2°C (Coolbear et al., 1983). Measurements at the same reduced temperatures were not available, but to allow for the comparison we chose the experiments with the nearest possible θ. For POPC this meant 0.18, but for DPPC the order parameter had been measured at 90°C (θ = 0.16) only for C2. Thus, the rest of the profile has been approximated based on the measurement at 60°C. It should be emphasized that this approximation can be used only to assess the general behavior of the order parameters as the decrease in the order parameters due to a higher temperature is not expected to be uniform along the chain.

The calculated order profile of the sn-2 chain of PLPC is compared with the ^{2}H NMR profile of PiLPC(16:0/18:2$^{\Delta 6,9}$) (Baenziger et al., 1991). PiLPC has the double bonds three carbons higher in the chain than the PLPC. Interestingly, at the position C6 of the sn-2 chain the comparison is possible with the measured order parameter of PLPC, because in the

synthetization of PiLPC specifically deuterated at C6, some PLPC was also formed, which gave its own resonance in the NMR spectra (Baenziger et al., 1991). It should be noted in the comparison that the experimental order parameters have been measured at lower θ than the one used in the simulation. Hence, the experimental order parameters might be somewhat smaller at the same θ as in the simulation, although it should be noted that this is not necessarily the case for all of the carbon segments (Baenziger et al., 1991).

The comparison of the order parameter profiles of the sn-1 chains at the approximately similar reduced temperatures (Fig. 10) suggests that, in general, the order increases with unsaturation. This has also been observed by ^{2}H NMR when comparing saturated and monounsaturated systems (Seelig and Seelig, 1977; Seelig and Browning, 1978; Paddy et al., 1985) and in the studies of polyunsaturated systems (McCabe et al., 1994). The major differences in the profiles appear in the region C2-C10, after which all profiles decrease monotonically.

The behavior of the C2 of the sn-1 chain in the simulation differs from the behavior generally observed in the experiments. Usually the order parameter for C2 is higher than the one for C3; this was also observed in the beginning of the simulation (Hyvönen et al., 1995). The continued simulation allowed us to assess the convergence behavior of the order parameters (Hyvönen et al., 1997), indicating that the rate of convergence slightly varied for the different carbon segments.

The shapes of the order parameter profiles in the beginning of the sn-1 chains (C4-C10) have been observed to be slightly different in the case of DPPC and POPC (Seelig and Seelig, 1977; Seelig and Browning, 1978). The difference in the profile shapes from DPPC to POPC reaches its maximum around C6, which has been interpreted as a local stiffening effect caused by the *cis* double bond (Seelig and Seelig, 1977; Seelig and Browning, 1978). From POPC to PLPC the effect tends to increase as the plateau extends. We interpret this to be due to the incorporation of one additional *cis* double bond, which causes the stiffening effect to influence more carbons in the sn-1 chain due to their occurrence at the same height in the bilayer (see Fig. 3). A similar idea has also been put forward based on the ^{2}H NMR experiments of lipid systems with varying degrees of unsaturation (Paddy et al., 1985; McCabe et al., 1994).

Comparison of the calculated order parameter profile of the sn-2 chains of PLPC (16:0/18:2$^{\Delta 9,12}$) with the experimental profile of PiLPC (16:0/18:2$^{\Delta 6,9}$) shows notable differences due to the different positions of the double bonds. If the three-carbon shift in the double bond positions is taken into account, the profiles of the regions C4-C11 and C7-C14 in PiLPC and PLPC, respectively, are remarkably similar. It is also interesting to note that the orientational order parameters for the methyl ends of the sn-2 chains for PiLPC and PLPC are almost equal. These comparisons suggest that the double bonds have very similar effects on the chain behavior despite the different positions. The calculated order parameter at the position C6 of PLPC is also in good accordance with the measured parameter, especially when the difference in θ is taken into account.

As already shown and discussed in more detail (Hyvönen et al., 1997), we have observed differences for some carbon segments between the orientational order parameters calculated as the average of $-S_j^{CD}$ parameters and the S_j^{mol}-based $-S_j^{CD}$ parameters. The differences indicated that the rotation of the carbon segments in the diunsaturated chains is remarkably restricted, but for the saturated chains only slight restrictions take place. The differences were noticed to be related to the inequivalence between the $-S_j^{CD}$ values for the CH_{aj} and CH_{bj}. The experimental observations of the inequivalence support these findings. In the sn-1 chains the inequivalence at the beginning of the chain is likely due to the connection to the rigid glycerol backbone, and the effect may also be enhanced by the double bonds. The relatively large inequivalence at carbons C6-C7 of the sn-1 chains is most likely due to the presence of the double bonds at the same height in the layer. The inequivalence in the beginning of the sn-2 chain is likely due to the tilted beginning conformation and at the double bond region by the restricted motional freedom caused by the rigid *cis* double bonds (Hyvönen et al., 1997).

Dihedral angle isomerization: gauche and trans states

The fraction of *gauche* states in the dihedral angles of the hydrocarbon chains was determined and is shown in Fig. 11. These fractions at the positions C4, C6, and C10 of DPPC have also been determined experimentally by infrared spectroscopy (Mendelsohn et al., 1989) and are shown for com-

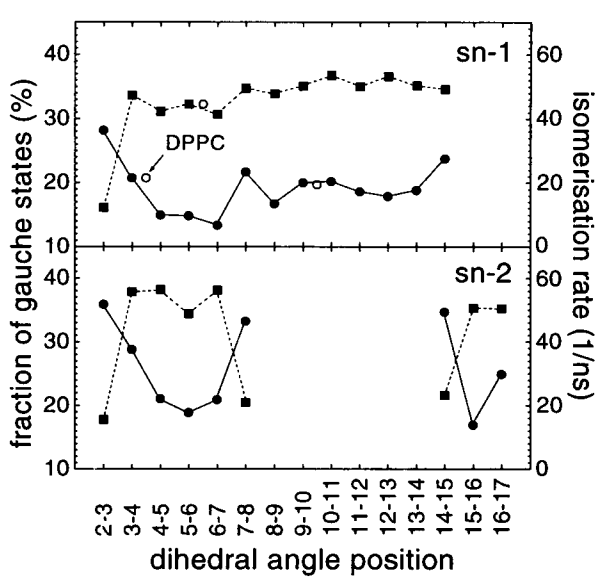

FIGURE 11 The fraction of *gauche* states (●) and isomerization rate (■) for the different dihedral angles of the chains. The fractions of the *gauche* states at the positions C4, C6, and C10 in a DPPC (16:0/16:0) system at 321 K obtained by infrared spectroscopy (Mendelsohn et al., 1989) are shown for comparison (○).

parison. In addition, the bond isomerization rate is given for each bond.

In the sn-1 chain, the C2-C3 bond has the largest fraction of *gauche* states, but interestingly, the same bond has the slowest isomerization rate. The smallest fraction of *gauche* bonds for the sn-1 chain is seen at the bond C6-C7, which together with the C4-C5 and C5-C6 bonds has also a slightly slower isomerization rate than the bonds at the end of the chain. It is seen that at C4 and C10 the *gauche* fractions in DPPC and PLPC are remarkably similar. At C6, which mostly resides at the same height in the PLPC bilayer as the double bonds, a considerable difference is found. This finding supports the idea that the region of the sn-1 chain lying at the same height with the double bonds is directly affected. The double bonds seem to reduce the fraction of *gauche* bonds and slightly slow down the isomerization rate. Both of these cause the order parameters of the respective segments to increase, as seen in Fig. 10.

Similar behavior as noticed for the C2-C3 bond of the sn-1 chain is also seen at the bonds C2-C3, C7-C8, and C14-C15 of the sn-2 chain; in the beginning of the chain and at both sides of the double bonds the *gauche* states are relatively common, but the isomerization rate is slow. Thus, the relatively small order parameters at C2 and C14 and the decrease from C7 to C8 are most likely structural effects due to the large fraction of *gauche* states and not due to the increased flexibility of the bonds. On average, 9.7 and 9.4% of the dihedral angles in the sn-1 chains were in g^+ and g^- states, respectively. Corresponding values for the sn-2 chains were 12.6 and 13.6%. The biggest differences between the fractions of g^+ and g^- states were at the dihedral angles C7-C8 and C8-C9 of the sn-1 chains and C2-C3, C6-C7, C7-C8, and C14-C15 of the sn-2 chains (data not shown).

The average fraction of *gauche* states from the measurements for C4, C6, and C10 in DPPC is 24.2% (Mendelsohn et al., 1989). The corresponding value for the PLPC from the simulation is 19.1%. The smaller value for the PLPC system is in accordance with the relatively high order parameters for the palmitoyl chain of PLPC and can be related to the existence of the two rigid double bonds. Similar effects have been noticed in the saturated chains of the PC molecules when cholesterol molecules are added. Thus, the effects of the double bonds of the sn-2 chains on the adjacent sn-1 chains may be comparable with the experimentally and theoretically noticed ordering effect of cholesterol molecules on the surrounding saturated chains, caused by the rigid ring system of the cholesterols (Dufourc et al., 1984; Davies et al., 1990; Scott, 1991; van der Sijs and Levine, 1994; Robinson et al., 1995). This is supported by the findings of Demel et al. (1972), that in a highly unsaturated system, (16:0/22:6)PC, the condensing effect of cholesterol was weak whereas in systems with lower unsaturation state, the condensing effect became more evident. These findings can be understood by an ordering effect of the double bonds on the saturated sn-1 chains that competes with the ordering effects caused by the cholesterol molecules. However, the analogy between unsaturation and cholesterol molecules does not hold in the case of permeability. The increased cholesterol content reduces the permeability of small molecules but only in systems where cholesterol causes condensation (Demel et al., 1972) whereas the incorporation of double bonds increases the permeability (Demel et al., 1972; van Deenen et al., 1972; Fettiplace and Haydon, 1980; Petersen, 1983; Stillwell et al., 1993). This is likely to be related to the direct role of double bonds in the permeation of small molecules, i.e., the possible ferry mechanism (Wiener and White, 1992; see above).

Root mean square fluctuations

The RMS fluctuations of the chain carbon segments as a function of the position in the y direction are shown in Fig. 12. A steepening increase of the dynamic fluctuations can be noticed toward the ends of both chains. Comparison of the segments of the sn-1 and sn-2 chains residing at the same height in the layer reveals that the sn-2 segments have larger dynamic fluctuations. It is notable, as seen in Fig. 3, that the beginning of the sn-2 chain has a narrower distribution than other chain segments in the bilayer normal direction, which reflects the fact that the fluctuations of these segments occur more in the directions of the bilayer plane than for the beginning of the sn-1 chain. For the sn-1 chain, the steepening increase is curvilinear, but for the sn-2 chain some slight variations take place at C1-C2 and C7 as well as C12-C13. These variations are likely to result from the tilted beginning and the double bonds, respectively. However, the variations are small compared with the general behavior of the RMS fluctuations in the sn-2 chains and were notable only at times during the simulation. Thus, they do not explain the small order parameters at the beginning and at the double bond region of the sn-2 chains.

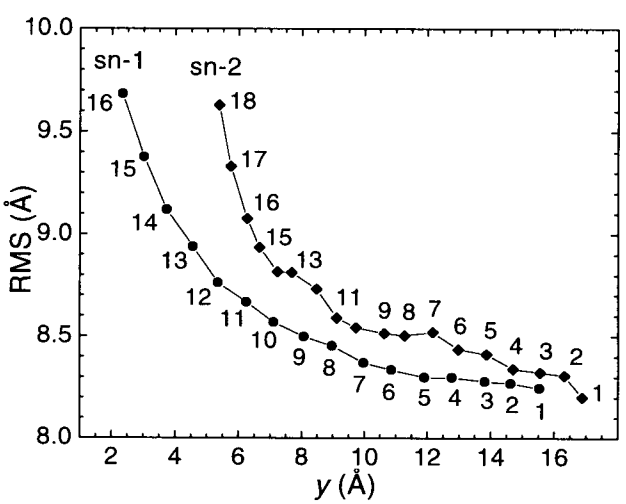

FIGURE 12 The root mean square fluctuations of the carbon segments in the sn-1 (●) and sn-2 (◆) chains as a function of their mean position along the bilayer normal.

Orientational distributions

The distributions of angles between a vector, e.g., a bond, and the bilayer normal were determined. The overall behavior of the chains is well described by the distributions of the angles between the vectors C1-C3 and the bilayer normal and between the vectors C1-C16 and C1-C18 and the bilayer normal. These distributions are shown in Fig. 13. The beginning of the sn-2 chain (C1-C3) has a narrower distribution than the sn-1 chain, which has more variety in the possible starting orientations. The most prevailing angle was approximately 24° for the sn-1 and 60° for the sn-2 chains, suggesting more parallel orientations with respect to the bilayer normal for the beginnings of the sn-1 than for the sn-2 chains.

The orientation distribution of the C1-C16 vector for the sn-1 chains is slightly narrower than the C1-C18 vector for the sn-2 chains. The most prevailing angle was 27° for the sn-1 and 38° for the sn-2 chains. It is interesting to note, however, that some chain conformations exist for which these vectors are almost perpendicular to the bilayer normal (Fig. 13); i.e., the chain end is close to the bilayer water interface. It is appealing to relate this observation to a general model for the peripheral attachment of proteins to lipid membranes based on the extended lipid conformations (Rytömaa and Kinnunen, 1995). The conformations where the chain end comes close to the water phase, as seen in the simulation, may provide a preliminary stage for the extended conformations and thus generally play a role in allowing interactions between the hydrophobic fatty acid chains and water-soluble molecules.

A more detailed picture of the orientational behavior in the chains is obtained from the distributions of the orientation angle for the CH_{aj} and CH_{bj} bonds. It was noticed that the CH_{aj} and CH_{bj} distributions differ more for the sn-2 chains than for the sn-1 chains, which is clearly related to the observed inequivalences between the S_j^{CD} values for the CH_{aj} and CH_{bj} (Hyvönen et al., 1997).

Structure of the double bond region

To monitor the orientation of the double bond region, the average distributions of the orientation angle were determined for the vectors C9-C10 and C12-C13 and are shown in Fig. 14. The time series of the orientation angle of these vectors for one of the PLPC molecules are also presented as an example. For the whole double bond region, the vector C9-C13, the tilt angle may vary from 0° to over 100°, and the most prevailing angle is ~37° (data not shown). The most common orientation angle of both double bonds is ~30°, but both can be found also in orientations near 90°; the second double bond has more of these perpendicular orientations than the first one. The time series of the orientation angle of the double bonds for the individual PLPC molecule reveal that in the 1-ns time scale the double bond orientation is able to change several times from a nearly parallel to a perpendicular orientation with respect to the bilayer normal (Fig. 14).

The angle distributions and time series of the dihedral angles C9-C10-C11-C12 and C10-C11-C12-C13 were determined for each PLPC molecule to monitor the internal structure of the double bond region. The angle distributions averaged over all molecules are shown in Fig. 15, in which the time series of one PLPC molecule is also given as an example. A jump movement between the angles of approximately ±120° is noticed for both dihedral angles. However, it is seen that the angles are not strictly ±120° but fluctuate by approximately ±40°. To determine the prevailing angles from the simulation, three classes of angles were used: +120 ± 60° (P), 0 ± 60° (intermediate), and −120 ±

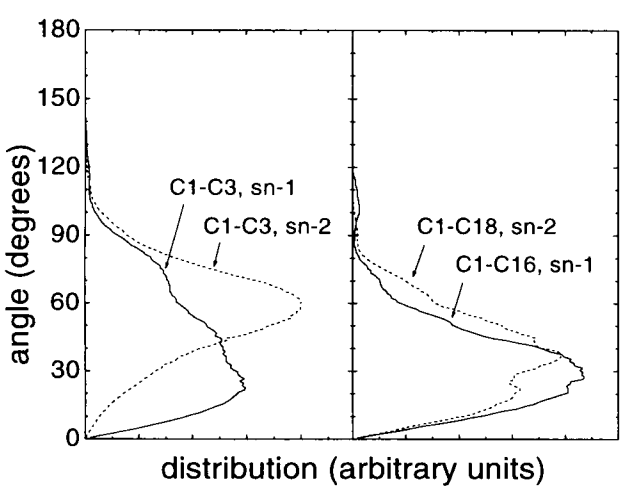

FIGURE 13 The distributions of the orientation angle between the C1-C3 (*left*) or C1-C16/C1-C18 (*right*) vectors and the bilayer normal for the sn-1 (——) and sn-2 (- - -) chains of the PLPC molecules. Note that here the direction of the bilayer normal is toward the bilayer center.

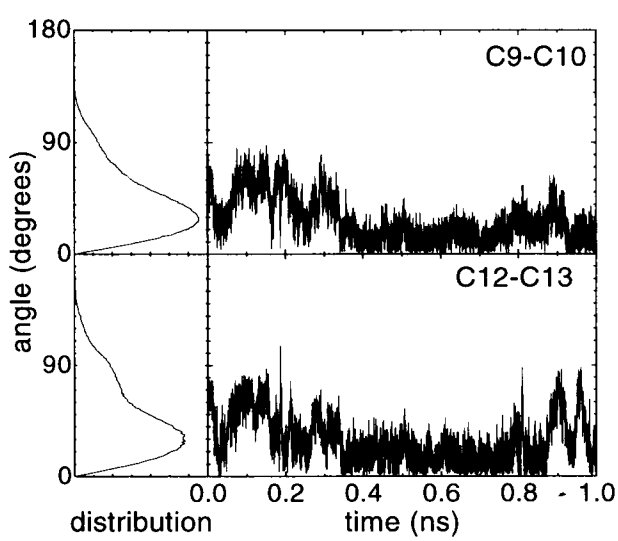

FIGURE 14 The distributions of the orientation angle (*left*) between the double bonds C9-C10 or C12-C13 and the bilayer normal together with the time series of the angle for one of the PLPC molecules (*right*). Note that here the direction of the bilayer normal is toward the bilayer center.

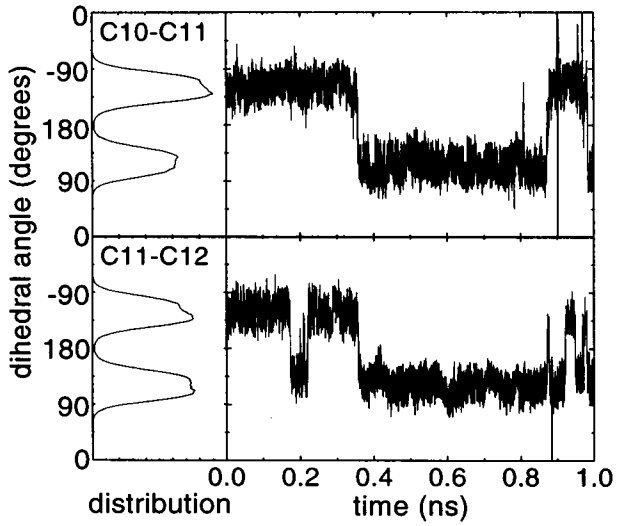

FIGURE 15 The distributions of the dihedral angles (*left*) over the bonds C10-C11 and C11-C12 of the sn-2 chains together with the time series of the dihedral angles for one of the PLPC molecules (*right*).

60° (M). The values of the dihedral angles determine the approximate angle between the double bond planes; the combinations +120 and +120 or −120 and −120° (PP/MM) end up with a nearly perpendicular orientation between the double bond planes whereas the combinations +120 and −120 or −120 and +120° (PM/MP) end up with the angle of ~60° between the double bond planes. In the simulation, 32.1% of the structures had the PP and 39.0% the MM combination. Furthermore, 9.3 and 19.0% of the conformations had the PM and MP combinations, respectively. The remaining 0.6% were in the intermediate states. The resulting structures are shown in Fig. 16, which also illustrates that the values of the dihedral angles between the double bonds determine whether the second double bond has the same orientation with respect to the bilayer normal

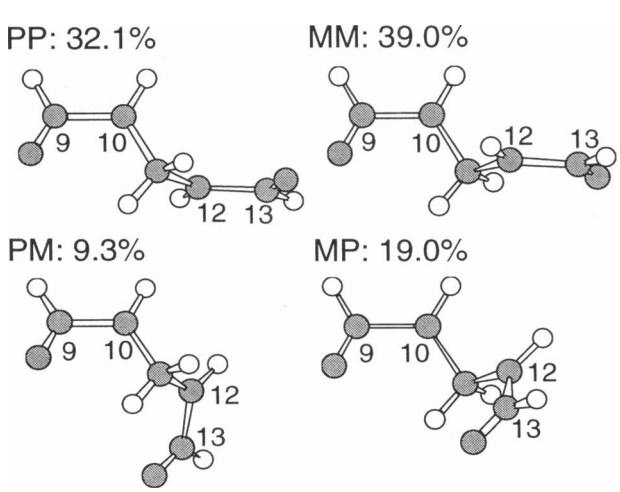

FIGURE 16 The four possible model conformations of the double bond region together with the percentage fraction of each conformation as found in the simulation of the PLPC bilayer.

as the first one or not. With the combinations PP and MM the orientation remains almost the same (71.1%), whereas with the PM or MP combinations the orientation changes 90–100° (28.3%). This explains the observed difference in the orientation angle distributions between the first and the second double bond (in Fig. 14). Applegate and Glomset (1986) have suggested four minimal energy conformations for 1,4-pentadiene (based on MM2 refinements), which had the dihedral angles of ±118° between the double bonds. These structures are in good accordance with the ones found in the present simulation for the double bond region. They also found the MM2 minima to be rather broad, which is consistent with the relatively large fluctuations observed in the simulation.

Based on ^{2}H NMR measurements, Baenziger et al. (1992) have suggested a model for the double bond region structure of PiLPC (16:0/18:2$^{\Delta 6,9}$). The model consists of two conformations between which a rapid movement takes place (correlation time of ~100 ps). The two model conformations are consistent with the main structures, PP and MM, of the simulation. It is interesting to note that they suggested the orientation of the double bond axes of PiLPC with respect to the bilayer normal to be similar to the orientations of the double bond axes in the crystal structure of linoleic acid (18:2$^{\Delta 9,12}$; Ernst et al., 1979), i.e., 45° (when the saturated segments of the chain are aligned parallel to the bilayer normal). This tilt is in reasonable agreement with the average tilt angles of the double bonds in the simulation, namely, 42.9° and 48.8° for C9-C10 and C11-C12, respectively. However, Baenziger et al. did not mention the possible occurrence of the PM and MP structures, which are seen in the simulation. As the model of Baenziger et al. for PiLPC did not achieve an exact fit with the experimental data, and still the S^{CD} parameter profiles of PiLPC and PLPC are remarkably similar at the double bond regions, the relatively rare occurrence of the PM and MP structures may also be found in real systems. In fact, the occurrence of the tilted conformations might be important for the permeability of small molecules; the tilt heavily disturbs the packing of the chains and may provide sufficient void volumes for small molecules to permeate. This leads to an idea that the main conformations in the membranes are vital for the stability of the system whereas the rarer ones offer opportunities for local events.

SUMMARY

Double bonds are known to play a crucial role in biomembranes. Our MD simulation for the diunsaturated PLPC (16:0/18:2$^{\Delta 9,12}$) bilayer is the first work that uses this biologically frequent fatty acid content of the phospholipids in a PC bilayer simulation. The results provided new structural and dynamic information on the effects of polyunsaturation on biological membranes. The given broad comparison of the computational results with existing experimental data corroborates the increasingly common conclusion that MD

simulations are able to reproduce consistent and valid information. Thus, they provide independent means to study biological macromolecular assemblies and, perhaps most importantly, a way to understand structure and function at the atomic level, a goal often far beyond experimental approaches.

It should be kept in mind, however, that the MD simulations on biomembranes are restrained with severe approximations both in the modeling and in the methodological side of the work. Particularly from the biochemical point of view, a simple PC bilayer is a rather naive description of a biological membrane. Thus, a lot of endeavor is needed to be able to build up computational model systems that more resemble their real counterparts, not only paying attention to the degree of unsaturation but also incorporating other structurally and functionally important lipid molecules as well as increasing the size of the system and the length of the simulations. From the methodological point of view, application of constant pressure and temperature algorithms together with improved treatment of the electrostatic interactions are important. As simulation of biomolecular systems is a new field of research, the techniques and algorithms are in a stage of continuous assessment and development. Together with the prosperous boost in the computational power by parallel architectures, biochemically more realistic and methodologically more advanced MD simulations on biomembranes are expected in the near future.

In all, the information content provided by the MD simulation data is enormous. Therefore, even though we have presented an extensive analysis of the 1-ns simulation, additional aspects still remain that have not been studied in detail, including such phenomena as hydrogen bonding network at the bilayer surface, motional correlations, electronic dipole potential across the bilayer, and the diffusion of lipid and water molecules. Those aspects were not included in the present analysis as we considered it necessary to first ensure the consistency of the model and focus on the structural effects of the double bonds, an area that has mostly been unexplored by computational methods operating at the atomic level. A brief summary of the present results is given below.

The hydrating water molecules appeared to be strongly oriented around the PLPC headgroup phosphorus atoms due to hydrogen bonding, but only weak orientation was observed around the nitrogen atoms. The dominating orientation of the water dipole moments at the bilayer surface was toward the bilayer interior. The most prevailing orientation of the phosphorus-nitrogen vector was 17° from the bilayer surface toward the water, which is in agreement with the general conclusion from the experimental studies that, on average, the PC headgroup is oriented almost parallel to the surface (Akutsu and Nagamori, 1991; Büldt and Wohlgemuth, 1981; Hauser et al., 1981; Seelig et al., 1977; Seelig and Seelig, 1980). The most prevailing orientation angle of the glycerol backbone was 25° from the bilayer normal. However, the distributions revealed that both the glycerol backbones and the PC headgroups had a variety of possible orientations. The most probable states for each dihedral angle, θ_1-θ_4/α_1-α_5, were $t\ g^+\ t\ g^-/t\ g^+\ g^+\ t\ g^-$. It is interesting to note that, when these dihedral angles occur in a single molecular conformation, one of the reported crystal structures of a DMPC molecule (Pascher et al., 1992) results. However, in the simulation only 5.8% of all the conformations had this type of sequence, and another crystal structure, $g^-\ t\ t\ g^-/t\ g^-\ g^-\ t\ g^+$, was even less prevalent (1.0%). This implies that in a liquid crystalline phase the glycerol backbones and the PC headgroups are apparently dynamic but not totally free; i.e., a relationship with the crystal structures still exists. Generally, the overall structure of the simulated PLPC bilayer was consistent with both experiments and membrane simulations for other systems.

Comparison of the orientational order parameter (S^{CD}) profile of the PLPC sn-1 chains with the experimental ones for DPPC and POPC systems at approximately the same reduced temperature suggested that the unsaturation increases the orientational order. Differences in the profile shapes were seen especially at the region C4-C10 and were interpreted as a stiffening effect due to the rigid *cis* double bonds approximately at the same height in the bilayer. The stiffening was also noticed from the inequivalence in the S^{CD} values of the methylene hydrogens at C6-C7 as well as in the low fraction of *gauche* bonds around C6 compared with a DPPC system and in the relatively low bond isomerization rate. It is notable that the S^{CD} values resulting for the sn-2 chains from the PLPC simulation are remarkably similar with the experimental ones for a PiLPC (16:0/18:$2^{\Delta 6,9}$) membrane when the three-carbon shift of the double bond region is taken into account. Comparison with the experimental S^{CD} value at C6 of PLPC was also possible and was in good agreement with the corresponding parameter from the current PLPC simulation. Moreover, in the beginning of the sn-2 chain, and at the vicinity of the double bonds, the S^{CD} inequivalence of the methylene hydrogens was remarkable, the fraction of *gauche* states large, and the isomerization rate low. The RMS fluctuations had a steepening increase toward the bilayer center for both chains and cannot explain the low S^{CD} values, particularly at the beginning and at the double bond region of the sn-2 chain. Therefore, the low S^{CD} values are most likely mainly caused by the local effects of the rigid *cis* double bonds and of the tilted chain beginnings on the bond isomerization.

The most prevailing orientation angle of the double bond region with respect to the bilayer normal was 37°. The internal structure of the double bond region was investigated in detail to find out whether the conformations proposed by Baenziger et al. (1992) in a case of a PiLPC system would be observed in the simulation. It was found that the conformations of the two-state model of Baenziger et al. represented the populations of 32 and 39% of all the conformations in the simulation. These two conformations, PP and MM, are characterized by the two torsion angles between the double bonds, +120 and +120° and −120 and −120°, respectively. In the simulation two other conforma-

tions, PM and MP, also existed but with lower populations of 9 and 19%, respectively. In the two dominating conformations the orientation of the two double bonds with respect to the bilayer normal is approximately the same. In the other two, the orientation of the second double bond is nearly perpendicular to the first one, thus affecting the packing of the layer quite dramatically. However, the existence of such conformations might be necessary to explain the role of double bonds in the increased permeability of the small molecules. Based on these findings it is also tempting to suppose more generally that the main conformations will typically function to stabilize the membrane structure, but the rarer ones are likely to have a prominent role in the proper (local) functioning of the membrane.

We are grateful to Dr. A. MacKerell, Jr. (University of Maryland) for providing the force field parameters. Professor Jukka Jokisaari and Dr. Juha Vaara are acknowledged for helpful discussions and for critical comments on the manuscript. Dr. Pentti Somerharju is also acknowledged for interesting discussions. The Center for Scientific Computing (Espoo, Finland) is acknowledged for computer resources.

This work was supported by the Academy of Finland and grants from the Jenny and Antti Wihuri (M.T. Hyvönen), Vilho, Yrjö, and Kalle Väisälä (M.T. Hyvönen), and Finnish Cultural Foundation (M.T. Hyvönen) and the Finnish Academy of Sciences (M. Ala-Korpela).

REFERENCES

Akutsu, H., and T. Nagamori. 1991. Conformational analysis of the polar headgroup in phosphatidylcholine bilayers: a structural change induced by cations. *Biochemistry.* 30:4510–4516.

Alper, H. E., D. Bassolino-Klimas, and T. R. Stouch. 1993. The limiting behavior of water hydrating a phospholipid monolayer: a computer simulation study. *J. Chem. Phys.* 99:5547–5559.

Applegate, K. R., and J. A. Glomset. 1986. Computer-based modeling of the conformation and packing properties of docosahexaenoic acid. *J. Lipid Res.* 27:658–680.

Baenziger, J. E., H. C. Jarrell, R. J. Hill, and I. C. P. Smith. 1991. Average structural and motional properties of a diunsaturated acyl chain in a lipid bilayer: effects of two *cis*-unsaturated double bonds. *Biochemistry.* 30: 894–903.

Baenziger, J. E., H. C. Jarrell, and I. C. P. Smith. 1992. Molecular motions and dynamics of a diunsaturated acyl chain in a lipid bilayer: implications for the role of polyunsaturation in biological membranes. *Biochemistry.* 31:3377–3385.

Bassolino-Klimas, D., H. E. Alper, and T. R. Stouch. 1993. Solute diffusion in lipid bilayer membranes: an atomic level study by molecular dynamics simulation. *Biochemistry.* 32:12624–12637.

Bassolino-Klimas, D., H. E. Alper, and T. R. Stouch. 1995. Mechanism of solute diffusion through lipid bilayer membranes by molecular dynamics simulation. *J. Am. Chem. Soc.* 117:4118–4129.

Bechinger, B., and J. Seelig. 1991. Conformational changes of the phosphatidylcholine headgroup due to membrane dehydration: a ^{2}H-NMR study. *Chem. Phys. Lipids.* 58:1–5.

Bicknell-Brown, E., K. G. Brown, and W. B. Person. 1982. Conformation-dependent Raman bands of phospholipid surfaces. *J. Raman Spectr.* 12:180–189.

Brooks, B. R., R. E. Bruccoleri, B. D. Olafson, D. J. States, S. Swaminathan, and M. Karplus. 1983. CHARMM: a program for macromolecular energy, minimization, and dynamics calculations. *J. Comput. Chem.* 4:187–217.

Brooks, C. L. III, M. Karplus, and B. M. Pettitt. 1988. Proteins: a theoretical perspective of dynamics, structure and thermodynamics. Adv. Chem. Phys. Vol. 71. Wiley-Interscience, New York.

Büldt, G., and R. Wohlgemuth. 1981. The headgroup conformation of phospholipids in membranes. *J. Membr. Biol.* 58:81–100.

Chiu, S.-W., M. Clark, V. Balaji, S. Subramaniam, H. L. Scott, and E. Jakobsson. 1995. Incorporation of surface tension into molecular dynamics simulation of an interface: a fluid phase lipid bilayer membrane. *Biophys. J.* 69:1230–1245.

Coolbear, K. P., C. B. Berde, and K. M. W. Keough. 1983. Gel to liquid-crystalline phase transitions of aqueous dispersions of polyunsaturated mixed-acid phosphatidylcholines. *Biochemistry.* 22:1466–1473.

Cullis, P. R., and M. J. Hope. 1985. Physical properties and functional roles of lipids in membranes. *In* Biochemistry of lipids and membranes. D. E. Vance and J. E. Vance, editors. Benjamin/Cummings Publishing, Menlo Park, CA. 25–72.

Damodaran, K. V., and K. M. Merz, Jr. 1994. A comparison of DMPC- and DLPE-based lipid bilayers. *Biophys. J.* 66:1076–1087.

Damodaran, K. V., K. M. Merz, Jr., and B. P. Gaber. 1995. Interaction of small peptides with lipid bilayers. *Biophys. J.* 69:1299–1308.

Davies, M. A., H. F. Schuster, J. W. Brauner, and R. Mendelsohn. 1990. Effects of cholesterol on conformational disorder in dipalmitoylphosphatidylcholine bilayers: a quantitative IR study of the depth dependence. *Biochemistry.* 29:4368–4373.

Demel, R. A., W. S. M. Geurts van Kessel, and L. L. M. van Deenen. 1972. The properties of polyunsaturated lecithins in monolayers and liposomes and the interactions of these lecithins with cholesterol. *Biochim. Biophys. Acta.* 266:26–40.

Dufourc, E. J., E. J. Parish, S. Chitrakorn, and I. C. P. Smith. 1984. Structural and dynamical details of cholesterol-lipid interaction as revealed by deuterium NMR. *Biochemistry.* 23:6062–6071.

Edholm, O., O. Berger, and F. Jähnig. 1995. Structure and fluctuations of bacteriorhodopsin in the purple membrane: a molecular dynamics study. *J. Mol. Biol.* 250:94–111.

Egberts, E., S.-J. Marrink, and H. J. C. Berendsen. 1994. Molecular dynamics simulation of a phospholipid membrane. *Eur. Biophys. J.* 22:423–436.

Eklund, K. K., J. A. Virtanen, P. K. J. Kinnunen, J. Kasurinen, and P. J. Somerharju. 1992. Conformation of phosphatidylcholine in neat and cholesterol-containing liquid-crystalline bilayers: application of a novel method. *Biochemistry.* 31:8560–8565.

Ernst, J., W. S. Sheldrick, and J.-H. Fuhrhop. 1979. Die Strukturen der essentiellen ungesättigten Fettsäuren, Kristallstruktur der Linolsäure sowie Hinweise auf die Kristallstrukturen der α-Linolensäure und der Arachidonsäure. *Z. Naturforsch.* 34b:706–711.

Essmann, U., L. Perera, and M. L. Berkowitz. 1995. The origin of the hydration interaction of lipid bilayers from MD simulation of dipalmitoylphosphatidylcholine membranes in gel and liquid crystalline phases. *Langmuir.* 11:4519–4531.

Esterbauer, H., M. Dieber-Rotheneder, G. Waeg, G. Striegl, and G. Jürgens. 1990. Biochemical, structural, and functional properties of oxidized low-density lipoprotein. *Chem. Res. Toxicol.* 3:77–92.

Fettiplace, R., and D. A. Haydon. 1980. Water permeability of lipid membranes. *Physiol. Rev.* 60:510–550.

Gally, H. U., W. Niederberger, and J. Seelig. 1975. Conformation and motion of the choline head group in bilayers of dipalmitoyl-3-sn-phosphatidylcholine. *Biochemistry.* 14:3647–3652.

Gawrisch, K., D. Ruston, J. Zimmerberg, V. A. Parsegian, R. P. Rand, and N. Fuller. 1992. Membrane dipole potentials, hydration forces, and the ordering of water at membrane surfaces. *Biophys. J.* 61:1213–1223.

Hauser, H., I. Pascher, R. H. Pearson, and S. Sundell. 1981. Preferred conformation and molecular packing of phosphatidylethanolamine and phosphatidylcholine. *Biochim. Biophys. Acta.* 650:21–51.

Hauser, H., I. Pascher, and S. Sundell. 1988. Preferred conformation and dynamics of the glycerol backbone in phospholipids: an NMR and x-ray single-crystal analysis. *Biochemistry.* 27:9166–9174.

Heller, H., M. Schaefer, and K. Schulten. 1993. Molecular dynamics simulation of a bilayer of 200 lipids in a gel and in the liquid-crystal phases. *J. Phys. Chem.* 97:8343–8360.

Hirshfeld, F. L. 1977. Bonded-atom fragments for describing molecular charge densities. *Theor. Chim. Acta.* 44:129–138.

Holte, L. L., S. A. Peter, T. M. Sinnwell, and K. Gawrisch. 1995. ^{2}H nuclear magnetic resonance order parameter profiles suggest a change of

molecular shape for phosphatidylcholines containing a polyunsaturated acyl chain. *Biophys. J.* 68:2396–2403.

Huang, P., J. J. Perez, and G. H. Loew. 1994. Molecular dynamics simulations of phospholipid bilayers. *J. Biomol. Struct. Dyn.* 11: 927–956.

Hyvönen, M., M. Ala-Korpela, J. Vaara, T. T. Rantala, and J. Jokisaari. 1995. Effects of two double bonds on the hydrocarbon interior of a phospholipid bilayer. *Chem. Phys. Lett.* 246:300–306.

Hyvönen, M., M. Ala-Korpela, J. Vaara, T. T. Rantala, and J. Jokisaari. 1997. Inequivalence of single CH_a and CH_b methylene bonds in the interior of a diunsaturated lipid bilayer from a molecular dynamics simulation. *Chem. Phys. Lett.* 268:55–60.

Jorgensen, W. L., J. Chandrasekhar, J. D. Madura, R. W. Impey, and M. L. Klein. 1983. Comparison of simple potential functions for simulating liquid water. *J. Chem. Phys.* 79:926–935.

Laaksonen, L. 1992. A graphics program for the analysis and display of molecular dynamics trajectories. *J. Mol. Graphics.* 10:33–34.

Lafleur, M., P. R. Cullis, and M. Bloom. 1990. Modulation of the orientational order profile of the lipid acyl chain in the L_α phase. *Eur. Biophys. J.* 19:55–62.

Lafleur, M., B. Fine, E. Sternin, P. R. Cullis, and M. Bloom. 1989. Smoothed orientational order profile of lipid bilayers by ^{2}H-nuclear magnetic resonance. *Biophys. J.* 56:1037–1041.

Lehtonen, J. Y. A., and P. K. J. Kinnunen. 1994. Changes in the lipid dynamics of liposomal membranes induced by poly(ethylene glycol): free volume alterations revealed by inter- and intramolecular excimer-forming phospholipid analogs. *Biophys. J.* 66:1981–1990.

Lewis, B. A., and D. M. Engelman. 1983. Lipid bilayer thickness varies linearly with acyl chain length in fluid phosphatidylcholine vesicles. *J. Mol. Biol.* 166:211–217.

Litman, B. J., and D. C. Mitchell. 1996. A role for phospholipid polyunsaturation in modulating membrane protein function. *Lipids.* 31(Suppl): 193–197.

Marrink, S.-J., and H. J. C. Berendsen. 1994. Simulation of water transport through a lipid membrane. *J. Phys. Chem.* 98:4155–4168.

Marrink, S.-J., M. Berkowitz, and H. J. C. Berendsen. 1993. Molecular dynamics simulation of a membrane/water interface: the ordering of water and its relation to the hydration force. *Langmuir.* 9:3122–3131.

McCabe, M. A., G. L. Griffith, W. D. Ehringer, W. Stillwell, and S. R. Wassall. 1994. ^{2}H NMR studies of isomeric ω3 and ω6 polyunsaturated phospholipid membranes. *Biochemistry.* 33:7203–7210.

McIntosh, T. J., and S. A. Simon. 1986. Hydration force and bilayer deformation: a reevaluation. *Biochemistry.* 25:4058–4066.

Mendelsohn, R., M. A. Davies, J. W. Brauner, H. F. Schuster, and R. A. Dluhy. 1989. Quantitative determination of conformational disorder in the acyl chains of phospholipid bilayers by infrared spectroscopy. *Biochemistry.* 28:8934–8939.

Merz, K. M. Jr., and B. Roux. 1996. Biological Membranes: A Molecular Perspective from Computation and Experiment. Birkhäuser, Boston.

Mouritsen, O. G., and P. K. J. Kinnunen. 1996. Role of lipid organization and dynamics for membrane functionality. *In* Biological Membranes: A Molecular Perspective from Computation and Experiment. K. M. Merz, Jr., and B. Roux, editors. Birkhäuser, Boston. 463–502.

Niebylski, C. D., and N. Salem, Jr. 1994. A calorimetric investigation of a series of mixed-chain polyunsaturated phosphatidylcholines: effect of sn-2 chain length and degree of unsaturation. *Biophys. J.* 67:2387–2393.

Op den Kamp, J. A. F., B. Roelofsen, and L. L. M. van Deenen. 1985. Structural and dynamic aspects of phosphatidylcholine in the human erythrocyte membrane. *Trends Biochem. Sci.* 8:320–323.

Paddy, M. R., F. W. Dahlquist, E. A. Dratz, and A. J. Deese. 1985. Simultaneous observation of order and dynamics at several defined positions in a single acyl chain using ^{2}H NMR of single acyl chain perdeuterated phosphatidylcholines. *Biochemistry.* 24:5988–5995.

Pascher, I., M. Lundmark, P.-G. Nyholm, and S. Sundell. 1992. Crystal structures of membrane lipids. *Biochim. Biophys. Acta.* 1113:339–373.

Petersen, D. C. 1983. The water permeability of the monoolein/triolein bilayer membrane. *Biochim. Biophys. Acta.* 734:201–209.

Robinson, A. J., W. G. Richards, P. J. Thomas, and M. M. Hann. 1994. Head group and chain behavior in biological membranes: a molecular dynamics computer simulation. *Biophys. J.* 67:2345–2354.

Robinson, A. J., W. G. Richards, P. J. Thomas, and M. M. Hann. 1995. Behavior of cholesterol and its effect on head group and chain conformations in lipid bilayers: a molecular dynamics study. *Biophys. J.* 68:164–170.

Roux, B., and M. Karplus. 1993. Ion transport in the gramicidin channel: free energy of the solvated right-handed dimer in a model membrane. *J. Am. Chem. Soc.* 115:3250–3262.

Rytömaa, M., and P. K. J. Kinnunen. 1995. Reversibility of the binding of cytochrome *c* to liposomes: implications for lipid-protein interactions. *J. Biol. Chem.* 270:3197–3202.

Schlenkrich, M., J. Brickmann, A. D. MacKerell, Jr., and M. Karplus. 1996. An empirical potential energy function for phospholipids: criteria for parameter optimisation and applications. *In* Biological Membranes: A Molecular Perspective from Computation and Experiment. K. M. Merz and B. Roux, editors. Birkhäuser, Boston. 31–82.

Scott, H. L. 1991. Lipid-cholesterol interactions: Monte Carlo simulations and theory. *Biophys. J.* 59:445–455.

Seelig, J., and J. L. Browning. 1978. General features of phospholipid conformation in membranes. *FEBS Lett.* 92:41–44.

Seelig, J., H.-U. Gally, and R. Wohlgemuth. 1977. Orientation and flexibility of the choline head group in phosphatidylcholine bilayers. *Biochim. Biophys. Acta.* 467:109–119.

Seelig, J., and W. Niederberger. 1974. Deuterium-labeled lipids as structural probes in liquid crystalline bilayers: a deuterium magnetic resonance study. *J. Am. Chem. Soc.* 96:2069–2072.

Seelig, A., and J. Seelig. 1977. Effect of a single *cis* double bond on the structure of a phospholipid bilayer. *Biochemistry.* 16:45–50.

Seelig, J., and A. Seelig. 1980. Lipid conformation in model membranes and biological membranes. *Q. Rev. Biophys.* 13:19–61.

Shinoda, W., T. Fukada, S. Okazaki, and I. Okada. 1995. Molecular dynamics simulation of the dipalmitoylphosphatidylcholine (DPPC) lipid bilayer in the fluid phase using the Nosé-Parrinello-Rahman NPT ensemble. *Chem. Phys. Lett.* 232:308–322.

Skarjune, R., and E. Oldfield. 1979. Physical studies of cell surface and cell membrane structure: determination of phospholipid head group organization by deuterium and phosphorus nuclear magnetic resonance spectroscopy. *Biochemistry.* 18:5903–5909.

Slater, S. J., M. B. Kelly, M. D. Yeager, J. Larkin, C. Ho, and C. D. Stubbs. 1996. Polyunsaturation in cell membranes and lipid bilayers and its effects on membrane proteins. *Lipids.* 31(Suppl):189–192.

Stillwell, W., W. Ehringer, and L. J. Jenski. 1993. Docosahexaenoic acid increases permeability of lipid vesicles and tumor cells. *Lipids.* 28: 103–108.

Stouch, T. R. 1993. Lipid membrane structure and dynamics studied by all-atom molecular dynamics simulations of hydrated phospholipid bilayers. *Mol. Simulation.* 10:335–362.

Sundaralingam, M. 1972. Discussion paper: Molecular structures and conformations of the phospholipids and sphingomyelins. *Ann. N.Y. Acad. Sci.* 195:324–355.

Tamm, L. K., and J. Seelig. 1983. Lipid solvation of cytochrome c oxidase: deuterium, nitrogen-14, and phosphorus-31 nuclear magnetic resonance studies on the phosphocholine head group and on *cis*-unsaturated fatty acyl chains. *Biochemistry.* 22:1474–1483.

Tu, K., D. J. Tobias, and M. L. Klein. 1995. Constant pressure and temperature molecular dynamics simulation of a fully hydrated liquid crystal phase dipalmitoylphosphatidylcholine bilayer. *Biophys. J.* 69: 2558–2562.

Ulrich, A. S., and A. Watts. 1994. Molecular response of the lipid headgroup to bilayer hydration monitored by ^{2}H-NMR. *Biophys. J.* 66: 1441–1449.

van Deenen, L. L. M., J. de Gier, and R. A. Demel. 1972. Relations between lipid compositon and permeability of membranes. *Biochem. Soc. Symp.* 35:377–382.

van der Sijs, D. A., and Y. K. Levine. 1994. A lattice dynamics model of lipid bilayer systems. *J. Chem. Phys.* 100:6783–6790.

van Gunsteren, W. F., and H. J. C. Berendsen. 1977. Algorithms for macromolecular dynamics and constraint dynamics. *Mol. Phys.* 34: 1311–1327.

Venable, R. M., Y. Zhang, B. J. Hardy, and R. W. Pastor. 1993. Molecular dynamics simulations of a lipid bilayer and of hexadecane: an investigation of membrane fluidity. *Science.* 262:223–226.

Wendoloski, J. J., S. J. Kimatian, C. E. Schutt, and F. R. Salemme. 1989. Molecular dynamics simulation of a phospholipid micelle. *Science.* 243:636–638.

Wiener, M. C., and S. H. White. 1992. Structure of a fluid dioleoylphosphatidylcholine bilayer determined by joint refinement of x-ray and neutron diffraction data. III. Complete structure. *Biophys. J.* 61: 434–447.

Wilson, M. A., and A. Pohorille. 1996. Mechanism of unassisted ion transport across membrane bilayers. *J. Am. Chem. Soc.* 118:6580–6587.